

SPARSE SPATIO TEMPORAL RECONSTRUCTION WITH CLOSABLE KERNEL SPACE

Anonymous authors

Paper under double-blind review

ABSTRACT

Quantifying spatio-temporal (ST) measures of dynamical systems is a crucial problem with wide ranging applications in climate modeling, epidemiology, physical processes to name a few. We are interested in the same but motivated by a rather practical scenario where sparse information is collected non-uniformly. To reconstruct the underlying dynamical system under such constraints, we propose a novel algorithm for learning the Koopman operator via a Reproducing Kernel Hilbert Space (RKHS) based on the *Laplacian Kernel Extended Dynamic Mode Decomposition* (Lap-KeDMD). We further show that our kernel space resolves a fundamental issue that is required for a faithful reconstruction of the Koopman operator of the underlying ST data by proving its closability. We demonstrate our method on standard benchmark cases – Burger’s Equation, fluid flow across cylinder and Duffing Oscillator. We then reconstruct the Koopman operator for a real ST Seattle traffic flow data that is collected non-uniformly. Necessary comparisons are made between the current state of the art kernel methods corresponding to Gaussian Radial Basis Function (GRBF) Kernel. Such empirical comparisons leads us to conclude that Lap-KeDMD remarkably outperforms as compared to that of aforementioned counter-part thereby, making the Laplacian Kernel a robust choice for such ST quantification.

1 INTRODUCTION

Spatio-temporal (ST) data have become ubiquitous in the current age where surveillance systems and sensors are recording large volumes of video data in airports, roads, weather monitoring etc. One important aspect of dealing with ST data is the task of prediction. Numerous applications in traffic prediction, video action recognition, anomaly detection have led to advancement in deep learning techniques like spatio-temporal convolution, spatio-temporal transformers, graph based spatio-temporal transformers to name a few (see, e.g. He et al. (2019) Zhou et al. (2016) Grigsby et al. (2021) Yu et al. (2020) Yan et al. (2021) Li et al. (2022)).

On the other hand, there is an increased focus on understanding ST data from a dynamical systems perspective (see Budišić et al. (2012)) where the task is not ST prediction but rather *spatio-temporal reconstruction*. Theoretical investigations of dynamical systems, first initiated by Poincare, has recently made huge advancements due to many applications arising in system design of engineered systems, optimization and control and understandings of complex physical phenomena like turbulence. Currently, data-driven methods provide a promising route in ST reconstruction by learning *spatio-temporal modes* of the dynamical system. One of the key and useful data-driven algorithm to provide ST modes is *Dynamic Mode Decomposition* developed by Schmid (2010). DMD in principle is an unsupervised machine learning (ML) algorithm Fujii & Kawahara (2019), based on *Krylov subspaces* Saad (2003) and *Arnoldi algorithm* Arnoldi (1951).

As far as ST reconstruction is concerned, ML architectures for instance Rubanova et al. (2019) (ODE-RNNs) or Ye et al. (2020); Murata et al. (2020); Hasegawa et al. (2020), (Brunton & Kutz, 2022, Chapter 6 Section 8, Page 236) based on Convolutional Neural Networks and Autoencoders offer a competitive platform to simulate, model and forecast complex, chaotic non-linear dynamical systems but face serious issues in analyzing the underlying dynamics as they lack tendency to operate or evolve with respect to *time* (cf. Mezić (2021); Sarker (2021); Haggerty et al. (2023)) Interestingly, such pitfall is overcome up by the data-driven techniques powered by the spectral analysis

of the infinite-dimensional linear Koopman operators (cf. Koopman (1931); Koopman & Neumann (1932); Mezić (2005)) over the underlying Hilbert space Williams et al. (2015a); Li et al. (2017) and such framework of DMD is referred as *Extended DMD* (eDMD). However, since such data driven methods are leveraged by the finite rank representations of the Koopman operators, which fails to be compact Singh & Kumar (1979), hence making the usual L^2 -Hilbert space incomprehensible.

In such cases, choosing (adequate) RKHSs for the action of Koopman operators to perform DMD naturally becomes a more justifiable options, which is called as *Kernel Extended DMD* (KeDMD) Baddoo et al. (2022); Klus et al. (2018; 2020); Rosenfeld et al. (2022) and is central to this paper. Recent investigation in KeDMD by Colbrook in (Colbrook, 2023, Page 44) recommends that one should choose the kernel function space so that the Koopman operator on the underlying RKHS is not just densely defined but also ‘*closable*’. However, coming up with such kernel spaces is non-trivial Ikeda et al. (2022b;a). Among the popular choices of the kernel functions, is GRBF Kernel (Steinwart et al., 2006, Page 4639) which not only just finds application in data-driven modeling but also in various ML platforms such as support vector machines and etc.

There is a growing interest of data predictions based on collecting ST-reconstructions via Koopman operators over the underlying RKHS. However, the problem of ST-reconstruction for data predictions while collecting snapshots irregularly is still under-investigated. Ideally, *full dataset* is needed to initiate DMD and is synthesis by stacking the data snapshots collected in a regular time-sampled manner. Experimental analysis in Bevanda et al. (2024); Tu et al. (2014); Klus et al. (2016); Rosenfeld et al. (2022); Brunton & Kutz (2022); Williams et al. (2015a); Schmid (2010; 2022); Baddoo et al. (2022) (and references there in) seems to enjoy such hypothetical-ideal situation, which seems to be quite far from the actual reality. Nevertheless, describing and forecasting the time evolution of dynamical systems still remains a challenging problem in the setting of limited irregularly placed data snapshots. Lack of investigation in this direction motivates this very paper, which provide the solution to this problem by leveraging Kernelized eDMD and novelty of Laplacian Kernel.

Recovering ST modes is essentially a key to the data-driven methods and fueled by this, this paper aims to provide the solution to the challenge of recovering data dynamics when we have irregular and sparse data in conjunction with limited dataset.

Our main contribution in the proposed work is summarized below:

1. We develop an RKHS by the Laplacian Kernel embedded as L^2 -Lebesgue measure in Subsubsection 3.1 and provide the Koopman operator theoretic quantification (cf. Theorem A.12 and Theorem A.19) of Koopman operators over this RKHS.
2. We show that the Koopman operators over this RKHS space is *closable* (Theorem 3.2) while showing that the current GRBF Kernel leads to a failure of closability. (Theorem 3.3).
3. We develop an algorithm to identify the Koopman operator over this RKHS based on irregular and sparsely sampled data and tabulate our results in Subsubsection 3.2. In particular, we showcase our results on real ST data collected sparsely from speed sensors in Seattle.

2 MATHEMATICAL BACKGROUND ON DYNAMICAL SYSTEM, KOOPMAN OPERATORS AND KERNEL SPACES

In reconstruction of ST data, we have Sampling-flow assumption that there is an underlying dynamical system and the data snapshots are a noisy observable of that dynamical system collected in certain sense. This particular assumption is common and standard to initiate the data-driven methods discussion and can be learned from Bevanda et al. (2024); Brunton & Kutz (2022); Colbrook (2023); Giannakis & Das (2020) with references present there in as well.

Assumption 2.1 (Sampling-flow assumption). *Let \mathcal{M} be a metric space and $\mathbf{F}_t : \mathcal{M} \rightarrow \mathcal{M}$ be the flow as defined in equation 1 along with the Borel-probability measure μ whose support $\text{supp } \mu = X$. Let the system be sampled at a fixed-time-instant, say $\Delta t (> 0)$ such that $\mathbf{F}_{n\Delta t} : \mathcal{M} \rightarrow \mathcal{M}$.*

$$\frac{d}{dt} \mathbf{x}(t) = \mathbf{f}(\mathbf{x}(t)) \implies \mathbf{F}_t(\mathbf{x}(t_0)) = \mathbf{x}(t_0) + \int_{t_0}^{t_0+t} \mathbf{f}(\mathbf{x}(t)) dt. \quad (1)$$

Definition 2.1 (Koopman Operators). Under [Assumption 2.1](#) the dynamical flow \mathbf{F}_t induces a linear map $\mathcal{K}_{\mathbf{F}_t}$ on the vector space of complex-valued functions on \mathcal{M} and on X defined as

$$\mathcal{K}_{\mathbf{F}_t} : L^2(\mu) \rightarrow L^2(\mu) \implies \mathcal{K}_{\mathbf{F}_t} g := g \circ \mathbf{F}_t. \quad (2)$$

We now provide definition of Koopman eigenfunction Φ_λ corresponding to eigenvalue $\lambda \in \mathbb{C}$ [Mezić \(2020\)](#).

Definition 2.2. Koopman eigenfunction $\Phi_\lambda \in C(\mathbb{X})$ satisfies $\Phi_\lambda(\mathbf{x}) = \exp(-\lambda t)\Phi_\lambda(\mathbf{F}_t(\mathbf{x}))$ over $t \in [0, T]$.

The sampling flow assumption give rise to the discrete dynamical system $(n, \mathcal{M}, \mathbf{F})$ based on which one can discuss the interaction of Koopman operator equation [4](#) and the snapshots of dynamic flow equation [3](#); these are respectively given as follows

Definition 2.3. Consider $(n, \mathcal{M}, \mathbf{F})$ be the discrete dynamical system where $n \in \mathbb{Z}$ is time $\mathcal{M} \subseteq \mathbb{R}^n$ is the state space and $\mathbf{x} \mapsto \mathbf{F}(\mathbf{x})$ is the dynamics. Then the data-set of snapshots of pairs corresponding to the discrete dynamical system $(n, \mathcal{M}, \mathbf{F})$ is given as following:

$$\underbrace{\begin{bmatrix} | & | & | & | \\ \mathbf{x}_1 & \mathbf{x}_2 & \cdots & \mathbf{x}_m \\ | & | & | & | \end{bmatrix}}_{\mathbf{X}} \xrightarrow{\mathbf{x}_i \mapsto \mathbf{F}(\mathbf{x}_i)} \underbrace{\begin{bmatrix} | & | & | & | \\ \mathbf{F}(\mathbf{x}_1) & \mathbf{F}(\mathbf{x}_2) & \cdots & \mathbf{F}(\mathbf{x}_m) \\ | & | & | & | \end{bmatrix}}_{\mathbf{X}^{\triangleright}} \stackrel{\mathbf{y}_i = \mathbf{F}(\mathbf{x}_i)}{:=} \begin{bmatrix} | & | & | & | \\ \mathbf{y}_1 & \mathbf{y}_2 & \cdots & \mathbf{y}_m \\ | & | & | & | \end{bmatrix}. \quad (3)$$

With a slight abuse of notation to the Koopman operator as \mathcal{K} (instead of $\mathcal{K}_{\mathbf{F}_t}$ in equation [2](#)), we understand that the Koopman operator acting on the observable $\phi : \mathcal{M} \subset \mathbb{C}^n \rightarrow \mathbb{C}$ as

$$\mathcal{K}\phi(\mathbf{x}_i) = \phi \circ \mathbf{F}(\mathbf{x}_i) = \phi(\mathbf{F}(\mathbf{x}_i)) = \phi(\mathbf{y}_i), \quad (4)$$

yields a brand new scalar valued function that gives the value of ϕ one-step ahead in the future against the discrete dynamical system $(n, \mathcal{M}, \mathbf{F})$, where $n \in \mathbb{Z}$, $\mathcal{M} \subseteq \mathbb{R}^N$ and $\mathbf{x} \mapsto \mathbf{F}(\mathbf{x})$. With data sets recorded in matrix \mathbf{X} and $\mathbf{X}^{\triangleright}$, the basic DMD based on singular value decomposition (SVD [Trefethen & Bau \(2022\)](#)) to provide the spectral-observables of \mathcal{K} is given in [Tu et al. \(2014\)](#).

In the natural interest of determining the Koopman spectra-observables i.e. Koopman eigen-values (μ_k) and Koopman eigen-functionals (φ_k) , they are also accompanied by the Koopman modes (ξ_k) of a certain vector valued observable $\mathbf{g} : \mathcal{M} \rightarrow \mathbb{R}^{N_o}$, $(N_o \in \mathbb{N})$, which is refer as the *full state observable* given as $\mathbf{g}(\mathbf{x}) = \mathbf{x}$. Further, one can have a following decomposition in terms of the aforementioned the triple *eigen-values, eigen-functionals & modes* of the Koopman operator corresponding to the (unknown) dynamics $\mathbf{x} \mapsto \mathbf{F}(\mathbf{x})$: $\mathbf{x} = \sum_{k=1}^{N_k} \zeta_k \varphi_k(\mathbf{x})$, $\mathbf{F}(\mathbf{x}) = \sum_{k=1}^{N_k} \mu_k \zeta_k \varphi_k(\mathbf{x})$, where, supposing that N_k is the number of tuples required for the re-construction of the system from the data of the dynamical system.

The eDMD is provided with the choice of scalar observables and for that let \mathcal{F} be the appropriate choice of scalar observables (such as RKHS). To do this, let $\psi_k : \mathcal{M} \rightarrow \mathbb{R}$ for $k = 1, \dots, N_k$ under the assumption that $\text{span}(\mathcal{F}_{N_k}) \subset \mathcal{F}$. In particular, the space of scalar observables is approximated using $\{\psi_k\}_{k=1}^{N_k}$ functions then feature space is \mathbb{R}^{N_k} . Additionally, the *feature map* ψ will be the ‘stacked’ column vector of entries $\{\psi_k\}$ given as $\psi(\mathbf{x}) = [\psi_1(\mathbf{x}) \ \psi_2(\mathbf{x}) \ \cdots \ \psi_{N_k}(\mathbf{x})]^\top$. With the feature space \mathbb{R}^{N_k} and considering the value of any functions $\phi, \tilde{\phi} \in \mathcal{F}_{N_k}$, where (again) $\text{span} \mathcal{F}_{N_k} \subset \mathbb{R}^{N_k}$, one can define the evaluation of both ϕ and $\tilde{\phi}$ against the inner product with certain coefficient vector \mathbf{a} and $\tilde{\mathbf{a}}$ in \mathbb{C}^{N_k} :

$$\phi(\mathbf{x}) = \langle \mathbf{a}, \psi(\mathbf{x}) \rangle_{\mathbb{R}^{N_k}} = \psi(\mathbf{x})^\top \mathbf{a}, \quad \tilde{\phi}(\mathbf{x}) = \langle \tilde{\mathbf{a}}, \psi(\mathbf{x}) \rangle_{\mathbb{R}^{N_k}} = \psi(\mathbf{x})^\top \tilde{\mathbf{a}}.$$

The goal of the eDMD is to employ the pair of data-set of snapshots defined in equation [3](#) to generate the compactified [1](#) version of the Koopman operator denoted by $\mathcal{K} \in \mathbb{R}^{N_k} \times \mathbb{R}^{N_k}$ for some given coefficients \mathbf{a} and $\tilde{\mathbf{a}}$ such that $\tau = (\mathcal{K}\phi - \tilde{\phi}) \in \mathcal{F}$, is minimum. The eDMD algorithm is given as:

¹finite rank representation of the infinite dimensional Koopman operator

Algorithm 1 Extended-DMD algorithm [Williams et al. \(2015a\)](#)

Step 1 With the pair of data-set of snapshots as defined in equation [3](#) compute following:

$$\Psi_x \triangleq [\psi(x_1) \ \psi(x_2) \ \cdots \ \psi(x_M)]; \Psi_y \triangleq [\psi(y_1) \ \psi(y_2) \ \cdots \ \psi(y_M)] \in \mathbb{R}^{M \times N_k}.$$

Step 2 Compute $\mathfrak{G} = \Psi_x^\top \Psi_x$ and $\mathbb{A} = \Psi_x^\top \Psi_y$.

Step 3 Determine pseudo-inverse of \mathfrak{G} . Denote it by $\mathfrak{G}^{(-)p}$.

Step 4 Determine \mathcal{K} by $\mathcal{K} \triangleq \mathfrak{G}^{(-)p} \mathbb{A}$.

In the spirit of SVD based DMD via [Schmid \(2010\)](#); [Tu et al. \(2014\)](#), the SVD of Ψ_x can be used to construct a matrix similar to \mathcal{K} ; this is given as follows:

Proposition 2.2. Let the SVD of Ψ_x be $\Psi_x \triangleq Q\Sigma Z^\top$, where Q and $\Sigma \in \mathbb{R}^{M \times M}$ and $Z \in \mathbb{R}^{N_k \times M}$. The pair of non-negative μ and \hat{v} are respective an eigenvalue and eigenvector of

$$\hat{\mathcal{K}} \triangleq \left(\Sigma^{(-)p} Q^\top \right) \left(\Psi_y \Psi_x^\top \right) \left(Q \Sigma^{(-)p} \right) = \left(\Sigma^{(-)p} Q^\top \right) \hat{\mathbb{A}} \left(Q \Sigma^{(-)p} \right), \quad (5)$$

if and only if μ and $v = Z\hat{v}$ are an eigen-value and eigen-vector of \mathcal{K} .

3 PROPOSED WORK

The choice of kernel functions can dramatically change the performance of ML routine [Singh \(2024\)](#); [Geifman et al. \(2020b\)](#), specifically in those situation when shorter training time or limited and sparse data is available. The most common kernel function that arises from the class of radial basis function (cf. [Fasshauer \(2007\)](#)) used in ML and AI routine such as speech enhancement is the class of *Laplace Kernel* given as follows:

$$K_{\text{EXP}}^{1,\sigma} \triangleq K_{\text{EXP}}^{1,\sigma}(\mathbf{x}, \mathbf{z}) := \exp\left(-\frac{\|\mathbf{x} - \mathbf{z}\|_2}{\sigma}\right) \quad \text{LAPLACE KERNEL.}$$

Laplace Kernel plays a critical role to characterize Deep Neural Tangent Kernel [Chen & Xu \(2021\)](#) and finds remarkable application in various ML tasks [Chen et al. \(2021a\)](#); [Ghojogh et al. \(2021\)](#); [Belkin et al. \(2018\)](#); [Geifman et al. \(2020b\)](#); [Genton \(2001\)](#). We are motivated by the works [Geifman et al. \(2020b\)](#), where they used the Laplacian Kernels to execute their ML task in presence of either partial data or sparse data. This is so because, loosely speaking we share the common theme of predicting the data based on limited sparse information. Lap-KeDMD algorithm to predict ST-modes with irregular and sparse data snapshots is given as:

Algorithm 2 Proposed Lap-KeDMD algorithm

Step 1 Construct limited data-set snapshots matrix which are collected in irregular and sparse manner.

Step 2 Compute Gram-Matrix $\mathfrak{G} := [\mathfrak{G}]_{i \times j}$ and Interaction-Matrix $\mathcal{I} := [\mathcal{I}]_{i \times j}$ by following:

$$[\mathfrak{G}]_{i \times j} = K_{\text{EXP}}^{1,\sigma}(\mathbf{x}_i, \mathbf{x}_j), \quad [\mathcal{I}]_{i \times j} = K_{\text{EXP}}^{1,\sigma}(\mathbf{y}_i, \mathbf{x}_j).$$

Step 3 Determine the spectral observables of the Gram-matrix \mathfrak{G} , i.e. Q and Σ .

Step 4 Construct $\hat{\mathcal{K}}$ via equation [5](#)

Reconstructed results from Step 4 in Algorithm [2](#) are yielded through the dominant Koopman modes calculated by the complex eigenvalues of the Gram Matrix whose real part's magnitude are comparatively larger helping in identifying the underlying patterns of the actual data of dynamical system. Dominant Koopman eigenvalues determined in such way is fundamentally important and thus plays a crucial role [Williams et al. \(2015b\)](#); [Baddoo et al. \(2022\)](#); [Mezić \(2021\)](#). Further, Koopman eigenvalues on an unit circle symbolizes the oscillatory mode of data, while on other hand, eigenvalues

lying inside an unit circle symbolizes decaying mode of data [Kutz et al. \(2016\)](#). We will compare the experimental results in [Subsubsection 3.2](#) generated by the Laplacian Kernel and the GRBF Kernel. To collect the experimental results from the GRBF Kernel, we execute the workflow of [Algorithm 2](#) by considering $[\mathcal{G}]_{i \times j} = K_{\text{EXP}}^{r^2, \sigma}(\mathbf{x}_i, \mathbf{x}_j)$, $[\mathcal{I}]_{i \times j} = K_{\text{EXP}}^{r^2, \sigma}(\mathbf{y}_i, \mathbf{x}_j)$.

3.1 CLOSABILITY RESULTS

For KeDMD methods, as already first noted by [Colbrook \(2023\)](#) and then also by [Giannakis & Valva \(2024\)](#) a challenge associated with RKHS techniques is that RKHS fails to exhibit invariance under the action of the Koopman operator. Further, Koopman operator invariance problem is actually tied with ST reconstruction of data matrix [Bevanda et al. \(2024\)](#) as well. The solution to this problem lies in choosing a suitable RKHSs where Koopman operators need to be closable [Ikeda et al. \(2022b\)](#). If in case closability criteria is not satisfied, this immediately will implicate that ST reconstruction is not possible. In the light of this, this section contains important theoretical results which leads up to the justification of closability of Koopman operators over the RKHS of Laplacian Kernel.

Throughout the paper, class of *observables functions* is captured by *holomorphic (entire) functions* ([Markushevich, 2005](#), Chapter 9) mapping between $\mathbb{C}^n \rightarrow \mathbb{C}$. In order to systematic define the Laplacian Kernel as an L^2 -measure, we consider an injective linear operator \mathfrak{J}_- over \mathbb{C}^n as $\mathfrak{J}_- \mathbf{z} = -\mathbf{I}_n \mathbf{z}$, where \mathbf{I}_n is the identity matrix. Define the graph of \mathfrak{J}_- as:

$$\begin{aligned} \text{--}\mathfrak{J}_+(\mathfrak{J}_-) &:= \{(\mathbf{z}, \mathfrak{J}_- \mathbf{z}) \in \mathbb{C}^n \times \mathbb{C}^n : \mathbf{z} \in \mathbb{C}^n\} \\ &= \{(\mathbf{z}, -\mathbf{z}) \in \mathbb{C}^n \times \mathbb{C}^n : \mathbf{z} \in \mathbb{C}^n\} \triangleq \text{--}\mathfrak{J}_+. \end{aligned} \quad (6)$$

Graph $\text{--}\mathfrak{J}_+$ introduced above will play a crucial role towards the end of paper in proving *closability* of Koopman operators. Laplacian Kernel as probability L^2 -measure $d\mu_{\sigma, 1, \mathbb{C}^n}(\mathbf{z}) \forall \sigma > 0$ is

$$d\mu_{\sigma, 1, \mathbb{C}^n}(\mathbf{z}) := \frac{1}{(2\pi\sigma^2)^n} K_{\text{EXP}}^{1, 2\sigma}(\text{--}\mathfrak{J}_+) dV(\mathbf{z}) = \frac{1}{(2\pi\sigma^2)^n} \exp\left(-\frac{\|\mathbf{z}\|_2}{\sigma}\right) dV(\mathbf{z}) \quad (7)$$

where $\|\mathbf{z}\|_2 = \sqrt{|z_1|^2 + \dots + |z_n|^2}$ for $\mathbf{z} = (z_1, \dots, z_n) \in \mathbb{C}^n$. Then, we can provide the inner product between two holomorphic functions $f : \mathbb{C}^n \rightarrow \mathbb{C}$ and $g : \mathbb{C}^n \rightarrow \mathbb{C}$ associated with this measure as

$$\langle f, g \rangle_{\sigma, 1, \mathbb{C}^n} := \frac{1}{(2\pi\sigma^2)^n} \int_{\mathbb{C}^n} f(\mathbf{z}) \overline{g(\mathbf{z})} e^{-\frac{\|\mathbf{z}\|_2}{\sigma}} dV(\mathbf{z}). \quad (8)$$

Now, that we have inner product, we can have following as the Hilbert function space corresponding to the same.

$$H_{\sigma, 1, \mathbb{C}^n} := \{\text{holomorphic function } f : \mathbb{C}^n \rightarrow \mathbb{C} : \|f\|_{\sigma, 1, \mathbb{C}^n} < \infty\}. \quad (9)$$

Hilbert space $H_{\sigma, 1, \mathbb{C}^n}$ equipped with the inner product equation [8](#) constitutes the RKHS (cf. Definition [A.1](#)) due to the existence of its orthonormal basis [Theorem A.3](#) by the virtue of [Theorem A.1](#).

Theorem 3.1. For $\sigma > 0$, let $\mathbf{z} = (z_1, \dots, z_n)$ and $\mathbf{w} = (w_1, \dots, w_n)$ be in \mathbb{C}^n . Then the reproducing kernel for RKHS $H_{\sigma, 1, \mathbb{C}^n}$ is

$$K_{\mathbf{w}}^{\sigma}(\mathbf{z}) = K^{\sigma}(\mathbf{z}, \mathbf{w}) := \left(\sqrt{\frac{\langle \mathbf{z}, \mathbf{w} \rangle_{\mathbb{C}^n}}{\sigma^2}}\right)^{-1} \cdot \sinh\left(\sqrt{\frac{\langle \mathbf{z}, \mathbf{w} \rangle_{\mathbb{C}^n}}{\sigma^2}}\right) \quad (10)$$

where $\langle \mathbf{z}, \mathbf{w} \rangle_{\mathbb{C}^n} = \mathbf{z} \mathbf{w}^{\top} = \sum_{i=1}^n z_i \overline{w_i}$.

Now that we have the RKHS $H_{\sigma, 1, \mathbb{C}^n}$, we are ready to define the Koopman operators \mathcal{K}_{φ} induced by holomorphic symbols $\varphi : \mathbb{C}^n \rightarrow \mathbb{C}^n$ over the RKHS $H_{\sigma, 1, \mathbb{C}^n}$. This definition fundamentally helps in operator theoretic quantification over the RKHS $H_{\sigma, 1, \mathbb{C}^n}$. It should be noted that, the way we exposed this definition is traditional follows from the setting of [Cowen \(1983\)](#); [Carswell et al. \(2003\)](#); [Cowen Jr \(2019\)](#); [Hai et al. \(2016\)](#); [Hai & Khoi \(2018\)](#); [Hai & Rosenfeld \(2021\)](#); [Le \(2014; 2017\)](#); [Gonzalez et al. \(2024\)](#).

Definition 3.1. Let $\varphi : \mathbb{C}^n \rightarrow \mathbb{C}^n$ be a holomorphic function in which every coordinate function of it are holomorphic functions from $\mathbb{C}^n \rightarrow \mathbb{C}$. Then, the Koopman operator induced by φ is denoted by $\mathcal{K}_{\varphi} : \mathcal{D}(\mathcal{K}_{\varphi}) \subset H_{\sigma, 1, \mathbb{C}^n} \rightarrow H_{\sigma, 1, \mathbb{C}^n}$ and is the linear operator defined by

$$\mathcal{K}_{\varphi}(f) := f \circ \varphi.$$

The domain of \mathcal{K}_{φ} is $\mathcal{D}(\mathcal{K}_{\varphi})$ given as $\mathcal{D}(\mathcal{K}_{\varphi}) := \{f \in H_{\sigma, 1, \mathbb{C}^n} : f \circ \varphi \in H_{\sigma, 1, \mathbb{C}^n}\}$.

Detailed Koopman operator theoretic quantification in terms of *boundedness* and *compactness* along with its proofs are provided in [Subsubsection A.5](#) and [Subsubsection A.6](#). Now, we will discuss the closability of the Koopman operators over the RKHS $H_{\sigma,1,\mathbb{C}^n}$ and the RKHS of the GRBF Kernels. We reviewed the closability of linear (unbounded) operators in [Appendix B](#). Our workflow of showing the closability of the Koopman operators over the RKHS $H_{\sigma,1,\mathbb{C}^n}$ is based on [Lemma B.1](#). **Theorem 3.2.** *Let \mathcal{K}_φ acts boundedly over the RKHS $H_{\sigma,1,\mathbb{C}^n}$ with $\varphi(\mathbf{z}) = \mathbf{A}\mathbf{z} + \mathbf{b}$. Define a subsequence of $-\mathfrak{Z}_+$ by $-\mathfrak{Z}_{+,N}$ as*

$$-\mathfrak{Z}_{+,N} := \left\{ (\mathbf{z}_N, -\mathbf{z}_N) \in \mathbb{C}^n \times \mathbb{C}^n : \lim_{N \rightarrow \infty} \|\mathbf{z}_N\|_2 = 0 \text{ where } \mathbf{z} \in \mathbb{C}^n \right\}. \quad (11)$$

There exists a sequence \mathfrak{K}_N inside the RKHS $H_{\sigma,1,\mathbb{C}^n}$ as defined $\mathfrak{K}_N := \|\mathbf{z}_N\|_2 K^\sigma(-\mathfrak{Z}_{+,N})$ such that $\lim_{N \rightarrow \infty} \mathfrak{K}_N = 0$. Also, \mathcal{K}_φ is closable over the RKHS $H_{\sigma,1,\mathbb{C}^n}$ if $\mathbf{b} \equiv 0$, implying φ is linear in \mathbb{C}^n , that is $\varphi(\mathbf{z}) = \mathbf{A}\mathbf{z}$. Let $\varphi_{\mathbf{A}}(\mathbf{z}) := \mathbf{A}\mathbf{z}$, then $\lim_{N \rightarrow \infty} \mathcal{K}_{\varphi_{\mathbf{A}}}\mathfrak{K}_N = 0$.

Proof. See [Subsubsection B.1](#)

□

In order to discuss the closability of Koopman operators on the GRBF Kernel, we recall it as follows subsequently followed by its RKHS as well.

$$K_{\text{EXP}}^{2,\sigma} \triangleq K_{\text{EXP}}^{2,\sigma}(\mathbf{x}, \mathbf{z}) := \exp\left(-\frac{\|\mathbf{x} - \mathbf{z}\|_2^2}{\sigma}\right) \quad \text{GRBF KERNEL.}$$

Norm for the GRBF Kernel [Steinwart et al. \(2006\)](#); [Steinwart & Christmann \(2008\)](#) is

$$\|f\|_\sigma^2 := \frac{2^n \sigma^{2n}}{\pi^n} \int_{\mathbb{C}^n} |f(\mathbf{z})|^2 e^{\sigma^2 \sum_{i=1}^n (z_i - \bar{z}_i)^2} dV(\mathbf{z}), \quad (12)$$

where $dV(\mathbf{z})$ is the usual Lebesgue volume measure on $\mathbb{C}^n \equiv \mathbb{R}^{2n}$. RKHS for $K_{\text{EXP}}^{2,\sigma}(\mathbf{x}, \mathbf{z})$ is:

$$H_\sigma := \{f : \mathbb{C}^n \rightarrow \mathbb{C} : f \text{ is holomorphic and } \|f\|_\sigma < \infty\}. \quad (13)$$

Following theorem leverages the bounded Koopman operators over the RKHS H_σ defined in equation [13](#) whose result is borrowed from [Gonzalez et al. \(2024\)](#), Corollary 1, Page 8).

Theorem 3.3. *Let \mathcal{K}_φ be bounded on H_σ , then $\varphi = \mathbf{A}\mathbf{z} + \mathbf{b}$, where $\mathbf{A} \in \mathbb{C}^{n \times n}$ and $\mathbf{b} \in \mathbb{C}^n$. Recall the domain $-\mathfrak{Z}_+$ defined in equation [6](#) and the subspace $-\mathfrak{Z}_{+,N}$ given in equation [11](#). Then $\lim_{N \rightarrow 0} \|\mathbf{z}_N\|_2 K_{\text{EXP}}^{2,\sigma}(-\mathfrak{Z}_{+,N}) = 0$ but $\mathbf{z}_N K_{\text{EXP}}^{2,\sigma}(-\mathfrak{Z}_{+,N}) \notin H_\sigma$. Since the sequence $\left\{ \mathbf{z} K_{\text{EXP}}^{2,\sigma}(-\mathfrak{Z}_{+,N}) \right\}_N \notin H_\sigma$, hence \mathcal{K}_φ is not closable over the RKHS H_σ .*

Proof. See [Subsubsection B.2](#)

□

3.2 RESULTS

We consider a number of important *benchmark experiments* to investigate the performance of the proposed Lap-KeDMD algorithm under limited irregular and sparse data snapshots. These experiments find wide-range applications in real-world setting and have been used by various practitioners [Bevanda et al. \(2024\)](#); [Colbrook \(2023\)](#); [Colbrook & Townsend \(2024\)](#); [Baddoo et al. \(2022\)](#); [Bagheri \(2013\)](#); [Williams et al. \(2015a,b\)](#); [Rosenfeld et al. \(2022\)](#); [Gonzalez et al. \(2024\)](#).

However, previous work relied on the collection of spatio-temporal data in uniform time sampled manner. We consider the same benchmark experiments by irregularly sampling sparse data with the same goal of determining ST modes via the compacted Koopman operators achieved over the RKHS of Laplacian kernel ([Theorem A.19](#)) and GRBF kernels ([Gonzalez et al. \(2024\)](#)). Explanations are in the Appendix.

Additionally we consider a real-world spatio-temporal data collected from Seattle freeway traffic speed sensors (experiment 4). This dataset has innate irregularity and sparsity due to the placement of sensors. Moreover, there is no known underlying dynamical system generating this dataset. This makes the reconstruction of this data set extremely challenging. In every experiment, we compare

the spatio-temporal reconstruction using our proposed Laplacian Kernel $K_{\text{EXP}}^{1,1}$ (Algorithm 2) with the state-of-the art GRBF Kernel $K_{\text{EXP}}^{2,1}$ (replacing $K_{\text{EXP}}^{1,1}$ by $K_{\text{EXP}}^{2,1}$ in Algorithm 2).

Table 1: Governing equations of experiments (if available).

EXPERIMENT	GOVERNING EQUATION(S)
1.	$\frac{\partial u}{\partial t} + u \frac{\partial u}{\partial x} = \nu \frac{\partial^2 u}{\partial x^2}$
2.	$\frac{\partial}{\partial t} \mathbf{u}(x, y, t) + \mathbf{u}(x, y, t) \cdot \nabla \mathbf{u}(x, y, t) + \nabla p(x, y, t) - \frac{1}{\text{RE}} \nabla^2 \mathbf{u}(x, y, t) = 0.$
3.	$\dot{\mathbf{x}} = \mathbf{y}, \dot{\mathbf{y}} = -0.5\mathbf{y} + \mathbf{x} - \mathbf{x}^3.$
4.	n/a

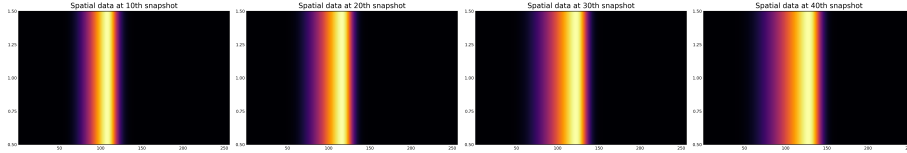


Figure 1: EXPERIMENT 1: *Nonlinear Burger's Equation*. Spatial evolution of 256 spatial values over the time span of $[0, 10]$ sec. Presented are the spatial data snapshots collected at the time stamp $10^{\text{th}}, 20^{\text{th}}, 30^{\text{th}}$ and 40^{th} .

Table 2: EXPERIMENT 1: *Nonlinear Burger's Equation*. ST reconstruction through dominant Koopman modes via $K_{\text{EXP}}^{1,1}$ and $K_{\text{EXP}}^{2,1}$ with irregular and sparse 40 snapshots out of actual 100 snapshots.

# KOOPMAN MODE	GROUND TRUTH	IRREGULAR & SPARSE	RECON. VIA LAP	RECON. VIA GRBF	KOOPMAN EIGENVALUES (LAP, GRBF)
# 39 th					$0.99 + 0i, 0.99 + 0i$

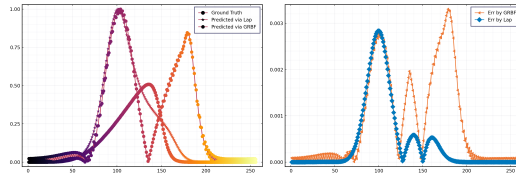


Figure 2: EXPERIMENT 1: *Nonlinear Burger's Equation*. Spatial reconstruction result along with ground truth for spatial data present at 39^{th} snapshot by both $K_{\text{EXP}}^{1,1}$ and $K_{\text{EXP}}^{2,1}$ (left). Absolute error plots for the same as well (right), where performance by $K_{\text{EXP}}^{2,1}$ is poor as compared to $K_{\text{EXP}}^{1,1}$.

378
379
380
381
382
383
384
385
386
387
388
389
390
391
392
393
394
395
396
397
398
399
400
401
402
403
404
405
406
407
408
409
410
411
412
413
414
415
416
417
418
419
420
421
422
423
424
425
426
427
428
429
430
431

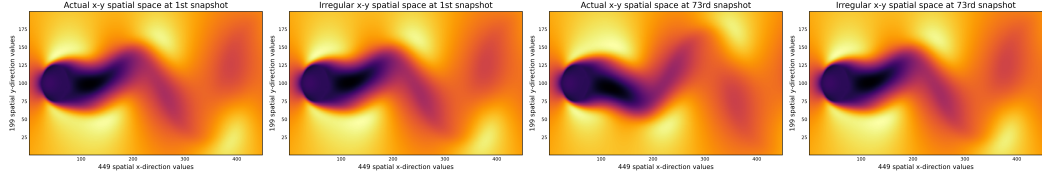


Figure 3: EXPERIMENT 2: *Fluid flow across cylinder*. A sample of 1st and 73rd snapshots out of available 151 snapshots for 2–D spatial plots of $x \times y \in \mathbb{R}^{449} \times \mathbb{R}^{199}$ spatial sensors values evolving with respect to time uniformly over time space $[1, 151]$ sec (scaled) in 1st and 3rd entries. Irregular and and sparse spatial 2–D plots of the same are given in 2nd and 4th entries respectively. Few of entries of uniform time sampling recorded by 151 time sensors (scaling) are $[1, 2, 3, \dots, 151]^T$ sec while on the other hand, the irregular version of the same is given as $[151, 148, 144, 9, 6, \dots, 94, 98, 97, 103]^T$ sec.

Table 3: EXPERIMENT 2: *Fluid flow across cylinder*. ST reconstruction through dominant Koopman modes via $K_{\text{EXP}}^{1,1}$ and $K_{\text{EXP}}^{2,1}$ with irregular and sparse 100 snapshots out of total 151 snapshots. Labeling for both spatial directions x and y is same from [Figure 3](#).

# KOOPMAN MODE	GROUND TRUTH	IRREGULAR & SPARSE	RECON. VIA LAP (REAL/IMAG)	RECON. VIA GRBF (REAL/IMAG)	KOOPMAN EIGENVALUES (LAP, GRBF)
# 99 th					$0.96 + 0i, 0.88 + 0i$

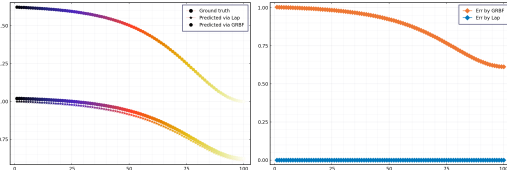


Figure 4: EXPERIMENT 2: *Fluid flow across cylinder*. Spatial reconstruction results along with ground truth for 2–D spatial data present at the 99th snapshot by both $K_{\text{EXP}}^{1,1}$ and $K_{\text{EXP}}^{2,1}$ (left). Absolute error plots for the same as well (right).

Governing 2–D equations for chaotic Duffing Oscillator is already given in entry 3 in [Table 1](#) Dataset for this experiment build by an initial condition given as $[-1.8760, 1.7868]^T$. This experiment actually belongs to the natural setting of phase-portrait reconstruction problem which we have adopted the same to test proposed Lap-KeDMD algorithm in terms of spatial-modes reconstruction.

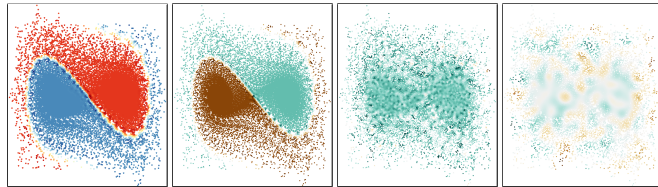


Figure 5: EXPERIMENT 3: *Duffing Oscillator*. Chaotic Duffing Oscillator with actual full dataset (ground truth in first entry), irregular and sparse of the same (second entry), prediction via $K_{\text{EXP}}^{1,1}$ (third entry) and prediction via $K_{\text{EXP}}^{2,1}$ (fourth entry) based on provided 35000 trajectories values.

432
433
434
435
436
437
438
439
440
441
442
443
444
445
446
447
448
449
450
451
452
453
454
455
456
457
458
459
460
461
462
463
464
465
466
467
468
469
470
471
472
473
474
475
476
477
478
479
480
481
482
483
484
485

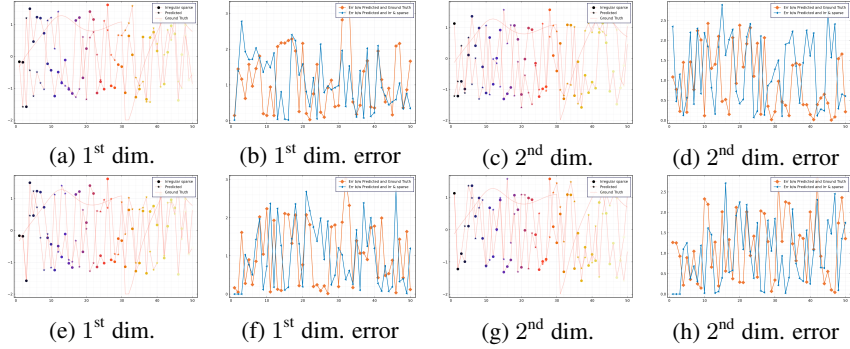


Figure 6: EXPERIMENT 3: *Duffing Oscillator*. State space reconstruction in both dimensions used for phase portraits reconstruction in entries third and fourth in Figure 5. First state space is $x \in \mathbb{R}^{35000}$ followed by second space $y \in \mathbb{R}^{35000}$. Reconstruction of these x and y by $K_{\text{EXP}}^{-1,1}$ are given in Figure 6a and Figure 6c. On the other hand, reconstruction of these x and y by $K_{\text{EXP}}^{1,1}$ are given in Figure 6e and Figure 6g. When we reconstruct and compare the complete phase portraits in third and fourth entries in Figure 5, we see that the result by $K_{\text{EXP}}^{1,1}$ outperforms the $K_{\text{EXP}}^{-2,1}$.

Table 4: EXPERIMENT 4: *Seattle I-5 Freeway Traffic Speed data*. ST reconstruction through dominant Koopman modes via $K_{\text{EXP}}^{-1,1}$ and $K_{\text{EXP}}^{2,1}$. For this experiment, real and imaginary parts of eigenvalues delivered by $K_{\text{EXP}}^{2,1}$ are in the order of $O(10^{-q})$, $q \gg 1$ due to ill-condition of Gram Matrix.

# KOOPMAN MODE	GROUND TRUTH	RECON. VIA LAP	RECON. VIA GRBF	KOOPMAN EIGENVALUES (LAP, GRBF)
# 23 th				$-0.28 - 0.46i, 0 + 0i$

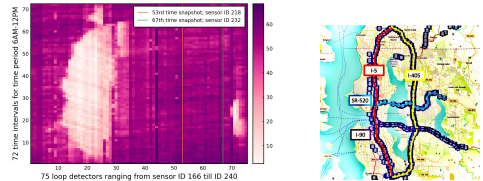


Figure 7: EXPERIMENT 4: *Seattle I-5 Freeway Traffic Speed data*. (Left) For the Seattle I-5 freeway traffic speed data, there are 75 loop detectors recording vehicle’s speed in a 72 time intervals frame over a rush-hour period 6:00 am — 12:00 pm; follow Cui et al. (2018; 2019) for more details. These 75 loop detectors present on freeway have sensor IDs as 166 till 240 in sequentially manner. (Right) Map of Seattle freeway from Cui et al. (2018; 2019) showing their inductive loop detector locations where each blue icon indicate loop detectors at every traffic sensor present at every milepost.

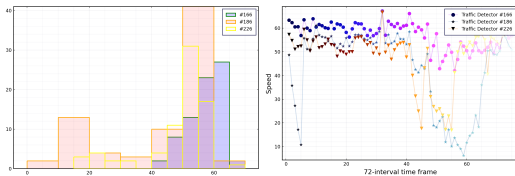


Figure 8: EXPERIMENT 4: *Seattle I-5 Freeway Traffic Speed data*. Histogram (speed vs. histogram bins) of speed data on Seattle I-5 freeway traffic speed data collected by sensors with loop detector IDs 166th, 186th and 226th (left). Plot of Seattle I-5 freeway speed collected on these sensors (right).

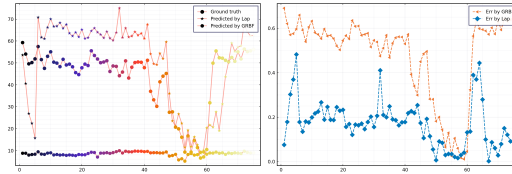
486
487
488
489
490
491492
493
494
495
496

Figure 9: EXPERIMENT 4: *Seattle I-5 Freeway Traffic Speed data*. Spatio-temporal speed reconstruction result along with the ground truth for speed data present at the Seattle I-5 freeway traffic sensor ID 218th by both $K_{\text{EXP}}^{-1,1}$ and $K_{\text{EXP}}^{-2,1}$ (left). Absolute error plots for the same as well (right). Speed data collected at the Seattle I-5 freeway sensor ID 218th corresponds to 53rd time snapshot.

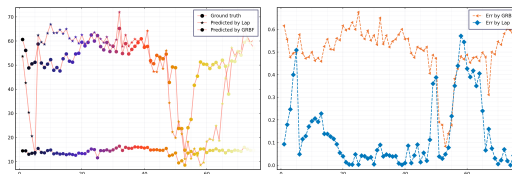
497
498
499
500
501
502
503504
505
506
507
508

Figure 10: EXPERIMENT 4: *Seattle I-5 Freeway Traffic Speed data*. Spatio-temporal speed reconstruction result along with the ground truth for speed data present at the Seattle I-5 freeway sensor ID 232th snapshot by both $K_{\text{EXP}}^{-1,1}$ and $K_{\text{EXP}}^{-2,1}$ (left). Absolute error plots for the same as well (right). Speed data collected at the Seattle I-5 freeway sensor ID 232nd corresponds to 67th time snapshot.

509

4 CONCLUSION

510

511

512

513

514

515

516

517

518

519

520

521

522

523

524

525

526

REFERENCES

527

528

529

530

531

532

533

534

535

536

537

538

539

Walter Edwin Arnoldi. The principle of minimized iterations in the solution of the matrix eigenvalue problem. *Quarterly of Applied Mathematics*, 9(1):17–29, 1951.

Nachman Aronszajn. Theory of reproducing kernels. *Transactions of the American Mathematical Society*, 68(3):337–404, 1950.

Peter J Baddoo, Benjamin Herrmann, Beverley J McKeon, and Steven L Brunton. Kernel learning for robust Dynamic Mode Decomposition: Linear and Nonlinear disambiguation optimization. *Proceedings of the Royal Society A*, 478(2260):20210830, 2022.

Shervin Bagheri. Koopman-mode decomposition of the cylinder wake. *Journal of Fluid Mechanics*, 726:596–623, 2013.

Mikhail Belkin, Siyuan Ma, and Soumik Mandal. To understand deep learning we need to understand kernel learning. In *International Conference on Machine Learning*, pp. 541–549. PMLR, 2018.

- 540 Petar Bevanda, Max Beier, Armin Lederer, Stefan Sosnowski, Eyke Hüllermeier, and Sandra Hirche.
541 Koopman kernel regression. *Advances in Neural Information Processing Systems*, 36, 2024.
542
- 543 Stephen P Boyd and Lieven Vandenbergh. *Convex optimization*. Cambridge University Press,
544 2004.
- 545 Steven L Brunton and J Nathan Kutz. *Data-driven science and engineering: Machine learning,*
546 *dynamical systems, and control*. Cambridge University Press, 2022.
547
- 548 Marko Budišić, Ryan Mohr, and Igor Mezić. Applied Koopmanism. *Chaos: An Interdisciplinary*
549 *Journal of Nonlinear Science*, 22(4), 2012.
- 550 Brent Carswell, Barbara D MacCluer, and Alex Schuster. Composition operators on the Fock space.
551 *Acta Sci. Math.(Szeged)*, 69(3-4):871–887, 2003.
552
- 553 Kai Chen, Twan van Laarhoven, and Elena Marchiori. Gaussian processes with skewed Laplace
554 spectral mixture kernels for long-term forecasting. *Machine Learning*, 110:2213–2238, 2021a.
- 555 Lin Chen and Sheng Xu. Deep neural tangent kernel and laplace kernel have the same {rkhs}. In
556 *International Conference on Learning Representations*, 2021. URL [https://openreview.](https://openreview.net/forum?id=vK9WrZ0QYQ)
557 [net/forum?id=vK9WrZ0QYQ](https://openreview.net/forum?id=vK9WrZ0QYQ).
- 558 Xinyu Chen, Mengying Lei, Nicolas Saunier, and Lijun Sun. Low-rank autoregressive tensor com-
559 pletion for spatiotemporal traffic data imputation. *IEEE Transactions on Intelligent Transporta-*
560 *tion Systems*, 23(8):12301–12310, 2021b.
561
- 562 Matthew J Colbrook. The Multiverse of Dynamic Mode Decomposition Algorithms. *arXiv preprint*
563 *arXiv:2312.00137*, 2023.
- 564 Matthew J Colbrook and Alex Townsend. Rigorous data-driven computation of spectral properties of
565 Koopman operators for dynamical systems. *Communications on Pure and Applied Mathematics*,
566 77(1):221–283, 2024.
567
- 568 John B Conway. *A Course in Functional Analysis*, volume 96. Springer, 2019.
- 569 Carl C Cowen. Composition operators on H^2 . *Journal of Operator Theory*, pp. 77–106, 1983.
570
- 571 Carl C Cowen Jr. *Composition operators on spaces of analytic functions*. Routledge, 2019.
- 572 Zhiyong Cui, Ruimin Ke, and Yinhai Wang. Deep Bidirectional and Unidirectional LSTM Recurrent
573 Neural Network for Network-wide Traffic Speed Prediction. *arXiv preprint arXiv:1801.02143*,
574 2018.
575
- 576 Zhiyong Cui, Kristian Henrikson, Ruimin Ke, and Yinhai Wang. Traffic graph convolutional recur-
577 rent neural network: A deep learning framework for network-scale traffic learning and forecast-
578 ing. *IEEE Transactions on Intelligent Transportation Systems*, 2019.
- 579 Gregory E Fasshauer. *Meshfree approximation methods with MATLAB*, volume 6. World Scientific,
580 2007.
581
- 582 Keisuke Fujii and Yoshinobu Kawahara. Supervised dynamic mode decomposition via multitask
583 learning. *Pattern Recognition Letters*, 122:7–13, 2019.
- 584 John Garnett. *Bounded Analytic Functions*, volume 236. Springer Science & Business Media, 2007.
585
- 586 Amnon Geifman, Abhay Yadav, Yoni Kasten, Meirav Galun, David Jacobs, and Basri
587 Ronen. On the Similarity between the Laplace and Neural Tangent Kernels. In
588 H. Larochelle, M. Ranzato, R. Hadsell, M.F. Balcan, and H. Lin (eds.), *Advances in Neu-*
589 *ral Information Processing Systems*, volume 33, pp. 1451–1461. Curran Associates, Inc.,
590 2020a. URL [https://proceedings.neurips.cc/paper_files/paper/2020/](https://proceedings.neurips.cc/paper_files/paper/2020/file/1006ff12c465532f8c574aeaa4461b16-Paper.pdf)
591 [file/1006ff12c465532f8c574aeaa4461b16-Paper.pdf](https://proceedings.neurips.cc/paper_files/paper/2020/file/1006ff12c465532f8c574aeaa4461b16-Paper.pdf).
- 592 Amnon Geifman, Abhay Yadav, Yoni Kasten, Meirav Galun, David Jacobs, and Basri Ronen. On
593 the similarity between the Laplace and Neural Tangent Kernels. *Advances in Neural Information*
Processing Systems, 33:1451–1461, 2020b.

- 594 Marc G Genton. Classes of kernels for machine learning: a statistics perspective. *Journal of Machine*
595 *Learning Research*, 2(Dec):299–312, 2001.
- 596
- 597 Benyamin Ghogh, Ali Ghodsi, Fakhri Karray, and Mark Crowley. Reproducing kernel hilbert
598 space, mercer’s theorem, eigenfunctions, nyström method, and use of kernels in machine learn-
599 ing: Tutorial and survey. *arXiv preprint arXiv:2106.08443*, 2021.
- 600 Dimitrios Giannakis and Suddhasattwa Das. Extraction and prediction of coherent patterns in in-
601 compressible flows through space–time Koopman analysis. *Physica D: Nonlinear Phenomena*,
602 402:132211, 2020.
- 603
- 604 Dimitrios Giannakis and Claire Valva. Consistent spectral approximation of Koopman operators
605 using resolvent compactification. *Nonlinearity*, 37(7):075021, 2024.
- 606 Efrain Gonzalez, Moad Abudia, Michael Jury, Rushikesh Kamalapurkar, and Joel A Rosenfeld.
607 The Kernel Perspective on Dynamic Mode Decomposition. *Transactions on Machine Learn-*
608 *ing Research*, 2024. ISSN 2835-8856. URL [https://openreview.net/forum?id=](https://openreview.net/forum?id=sIR8xv7hG1)
609 [sIR8xv7hG1](https://openreview.net/forum?id=sIR8xv7hG1).
- 610 Jake Grigsby, Zhe Wang, Nam Nguyen, and Yanjun Qi. Long-range transformers for dynamic
611 spatiotemporal forecasting. *arXiv preprint arXiv:2109.12218*, 2021.
- 612
- 613 David A Haggerty, Michael J Banks, Ervin Kamenar, Alan B Cao, Patrick C Curtis, Igor Mezić,
614 and Elliot W Hawkes. Control of soft robots with inertial dynamics. *Science robotics*, 8(81):
615 eadd6864, 2023.
- 616 Pham Viet Hai and Le Hai Khoi. Complex symmetric weighted composition operators on the Fock
617 space in several variables. *Complex Variables and Elliptic Equations*, 63(3):391–405, 2018.
- 618
- 619 Pham Viet Hai and Joel A Rosenfeld. Weighted Composition Operators on the Mittag-Leffler Spaces
620 of Entire Functions. *Complex Analysis and Operator Theory*, 15(1):1–26, 2021.
- 621
- 622 Pham Viet Hai et al. Boundedness and Compactness of Weighted Composition Operators on Fock
623 Spaces $F^p(\mathbb{C})$. *Acta Mathematica Vietnamica*, 41(3):531–537, 2016.
- 624 Brian C Hall. *Quantum theory for Mathematicians*. Springer, 2013.
- 625
- 626 Paul Richard Halmos. *A Hilbert space problem book*, volume 19. Springer Science & Business
627 Media, 2012.
- 628 Kazuto Hasegawa, Kai Fukami, Takaaki Murata, and Koji Fukagata. CNN-LSTM based reduced order
629 modeling of two-dimensional unsteady flows around a circular cylinder at different Reynolds
630 numbers. *Fluid Dynamics Research*, 52(6):065501, 2020.
- 631
- 632 Zhixiang He, Chi-Yin Chow, and Jia-Dong Zhang. Stcnn: A spatio-temporal convolutional neural
633 network for long-term traffic prediction. In *2019 20th IEEE International Conference on Mobile*
634 *Data Management (MDM)*, pp. 226–233, 2019. doi: 10.1109/MDM.2019.00-53.
- 635 Masahiro Ikeda, Isao Ishikawa, and Yoshihiro Sawano. Boundedness of composition operators on
636 reproducing kernel Hilbert spaces with analytic positive definite functions. *Journal of Mathemat-*
637 *ical Analysis and Applications*, 511(1):126048, 2022a.
- 638
- 639 Masahiro Ikeda, Isao Ishikawa, and Corbinian Schlosser. Koopman and Perron–Frobenius operators
640 on reproducing kernel Banach spaces. *Chaos: An Interdisciplinary Journal of Nonlinear Science*,
641 32(12), 2022b.
- 642 Stefan Klus, Péter Koltai, and Christof Schütte. On the numerical approximation of the Perron-
643 Frobenius and Koopman operator. *Journal of Computational Dynamics*, 3(1):51–79, 2016.
- 644
- 645 Stefan Klus, Andreas Bittracher, Ingmar Schuster, and Christof Schütte. A kernel-based approach
646 to molecular conformation analysis. *The Journal of Chemical Physics*, 149(24), 2018.
- 647
- 648 Stefan Klus, Feliks Nüske, and Boumediene Hamzi. Kernel-based approximation of the Koopman
649 generator and Schrödinger operator. *Entropy*, 22(7):722, 2020.

- 648 Bernard O Koopman. Hamiltonian systems and transformation in Hilbert space. *Proceedings of the*
649 *National Academy of Sciences*, 17(5):315–318, 1931.
- 650
- 651 Bernard O Koopman and J v Neumann. Dynamical systems of continuous spectra. *Proceedings of*
652 *the National Academy of Sciences*, 18(3):255–263, 1932.
- 653 J Nathan Kutz, Steven L Brunton, Bingni W Brunton, and Joshua L Proctor. *Dynamic Mode De-*
654 *composition: Data-Driven Modeling of Complex Dystems*. SIAM, 2016.
- 655
- 656 Trieu Le. Normal and isometric weighted composition operators on the Fock space. *Bulletin of the*
657 *London Mathematical Society*, 46(4):847–856, 2014.
- 658 Trieu Le. Composition operators between Segal–Bargmann spaces. *Journal of Operator Theory*, 78
659 (1):135–158, 2017.
- 660
- 661 Kunchang Li, Yali Wang, Peng Gao, Guanglu Song, Yu Liu, Hongsheng Li, and Yu Qiao. Uni-
662 former: Unified transformer for efficient spatiotemporal representation learning. *arXiv preprint*
663 *arXiv:2201.04676*, 2022.
- 664 Qianxiao Li, Felix Dietrich, Erik M Bollt, and Ioannis G Kevrekidis. Extended dynamic mode
665 decomposition with dictionary learning: A data-driven adaptive spectral decomposition of the
666 Koopman operator. *Chaos: An Interdisciplinary Journal of Nonlinear Science*, 27(10), 2017.
- 667
- 668 Alekseĭ Ivanovich Markushevich. *Theory of functions of a complex variable*, volume 296. American
669 Mathematical Soc., 2005.
- 670 Igor Mezić. Spectral properties of dynamical systems, model reduction and decompositions. *Non-*
671 *linear Dynamics*, 41:309–325, 2005.
- 672
- 673 Igor Mezić. Spectrum of the Koopman operator, spectral expansions in functional spaces, and state-
674 space geometry. *Journal of Nonlinear Science*, 30(5):2091–2145, 2020.
- 675 Igor Mezić. Koopman operator, geometry, and learning of dynamical systems. *Not. Am. Math. Soc.*,
676 68(7):1087–1105, 2021.
- 677
- 678 Takaaki Murata, Kai Fukami, and Koji Fukagata. Nonlinear mode decomposition with convolutional
679 neural networks for fluid dynamics. *Journal of Fluid Mechanics*, 882:A13, 2020.
- 680 Gert K Pedersen. *Analysis now*, volume 118. Springer Science & Business Media, 2012.
- 681
- 682 M Reed and B Simon. *Methods of modern mathematical physics. 1: Functional Analysis*. Academic
683 Press, April 1980.
- 684 Michael Reed. *Methods of modern mathematical physics: Functional Analysis*. Elsevier, 2012.
- 685
- 686 Joel A Rosenfeld, Rushikesh Kamalapurkar, L Forest Gruss, and Taylor T Johnson. Dynamic Mode
687 Decomposition for Continuous Time Systems with the Liouville operator. *Journal of Nonlinear*
688 *Science*, 32:1–30, 2022.
- 689 Yulia Rubanova, Ricky TQ Chen, and David K Duvenaud. Latent ordinary differential equations for
690 irregularly-sampled time series. *Advances in neural information processing systems*, 32, 2019.
- 691
- 692 Walter Rudin. Functional Analysis 2nd ed. *International Series in Pure and Applied Mathematics*.
693 *McGraw-Hill, Inc., New York*, 1991.
- 694 Yousef Saad. *Iterative methods for sparse linear systems*. SIAM, 2003.
- 695
- 696 Iqbal H Sarker. Deep learning: a comprehensive overview on techniques, taxonomy, applications
697 and research directions. *SN Computer Science*, 2(6):420, 2021.
- 698 Peter J Schmid. Dynamic Mode Decomposition of Numerical and Experimental Data. *Journal of*
699 *fluid mechanics*, 656:5–28, 2010.
- 700
- 701 Peter J Schmid. Dynamic Mode Decomposition and its variants. *Annual Review of Fluid Mechanics*,
54:225–254, 2022.

- 702 Joel H Shapiro. The essential norm of a composition operator. *Annals of mathematics*, pp. 375–404,
703 1987.
- 704 Himanshu Singh. Machine Learning Application of Generalized Gaussian Radial Basis Function
705 and Its Reproducing Kernel Theory. *Mathematics*, 12(6):829, 2024.
- 706 RK Singh and Ashok Kumar. Compact composition operators. *Journal of the Australian Mathe-*
707 *matical Society*, 28(3):309–314, 1979.
- 708 Elias M Stein and Rami Shakarchi. *Complex analysis*, volume 2. Princeton University Press, 2010.
- 709 Ingo Steinwart and Andreas Christmann. *Support vector machines*. Springer Science & Business
710 Media, 2008.
- 711 Ingo Steinwart, Don Hush, and Clint Scovel. An explicit description of the reproducing kernel
712 Hilbert spaces of Gaussian RBF kernels. *IEEE Transactions on Information Theory*, 52(10):
713 4635–4643, 2006.
- 714 Lloyd N Trefethen and David Bau. *Numerical linear algebra*. SIAM, 2022.
- 715 Jonathan H Tu, Clarence W Rowley, Dirk M Luchtenburg, Steven L Brunton, and J Nathan Kutz. ON
716 DYNAMIC MODE DECOMPOSITION: THEORY AND APPLICATIONS. *Journal of Computa-*
717 *tional Dynamics*, 1(2):391–421, 2014.
- 718 Matthew O Williams, Ioannis G Kevrekidis, and Clarence W Rowley. A data-driven approxima-
719 tion of the Koopman operator: Extending Dynamic Mode Decomposition. *Journal of Nonlinear*
720 *Science*, 25:1307–1346, 2015a.
- 721 Matthew O. Williams, Clarence W. Rowley, and Ioannis G. Kevrekidis. A kernel-based method
722 for data-driven Koopman spectral analysis. *Journal of Computational Dynamics*, 2(2):247–265,
723 2015b. ISSN 2158-2491. doi: 10.3934/jcd.2015005. URL [https://www.aims sciences.](https://www.aims sciences.org/article/id/ce535396-f8fe-4aa1-b6de-baaf986f6193)
724 [org/article/id/ce535396-f8fe-4aa1-b6de-baaf986f6193](https://www.aims sciences.org/article/id/ce535396-f8fe-4aa1-b6de-baaf986f6193).
- 725 Bin Yan, Houwen Peng, Jianlong Fu, Dong Wang, and Huchuan Lu. Learning spatio-temporal
726 transformer for visual tracking. In *Proceedings of the IEEE/CVF international conference on*
727 *computer vision*, pp. 10448–10457, 2021.
- 728 Shuran Ye, Zhen Zhang, Xudong Song, Yiwei Wang, Yaosong Chen, and Chenguang Huang. A flow
729 feature detection method for modeling pressure distribution around a cylinder in non-uniform
730 flows by using a convolutional neural network. *Scientific reports*, 10(1):4459, 2020.
- 731 Cunjun Yu, Xiao Ma, Jiawei Ren, Haiyu Zhao, and Shuai Yi. Spatio-temporal graph transformer
732 networks for pedestrian trajectory prediction. In *Computer Vision–ECCV 2020: 16th European*
733 *Conference, Glasgow, UK, August 23–28, 2020, Proceedings, Part XII 16*, pp. 507–523. Springer,
734 2020.
- 735 Shifu Zhou, Wei Shen, Dan Zeng, Mei Fang, Yuanwang Wei, and Zhijiang Zhang. Spa-
736 tial–temporal convolutional neural networks for anomaly detection and localization in crowded
737 scenes. *Signal Processing: Image Communication*, 47:358–368, 2016. ISSN 0923-5965. doi:
738 <https://doi.org/10.1016/j.image.2016.06.007>. URL [https://www.sciencedirect.com/](https://www.sciencedirect.com/science/article/pii/S0923596516300935)
739 [science/article/pii/S0923596516300935](https://www.sciencedirect.com/science/article/pii/S0923596516300935).
- 740 Kehe Zhu. *Spaces of Holomorphic Functions in the Unit Ball*, volume 226. Springer, 2005.

750 A APPENDIX

751 A.1 REPRODUCING KERNEL HILBERT SPACE

752 The definition of reproducing kernel Hilbert space (RKHS) is given as follows:

753 **Definition A.1.** Let $X = \emptyset$ and $(H, \langle \cdot, \cdot \rangle_H)$ be the Hilbert function space over X .